Search for nontensorial gravitational-wave backgrounds in the NANOGrav 15-year dataset

Zu-Cheng Chen,[1,2,3,4,§] Yu-Mei Wu,[5,6,*] Yan-Chen Bi,[6,7,†] and Qing-Guo Huang[5,6,7,‡]

[1]Department of Physics and Synergetic Innovation Center for Quantum Effects and Applications, Hunan Normal University, Changsha, Hunan 410081, China
[2]Institute of Interdisciplinary Studies, Hunan Normal University, Changsha, Hunan 410081, China
[3]Department of Astronomy, Beijing Normal University, Beijing 100875, China
[4]Advanced Institute of Natural Sciences, Beijing Normal University, Zhuhai 519087, China
[5]School of Fundamental Physics and Mathematical Sciences, Hangzhou Institute for Advanced Study, UCAS, Hangzhou 310024, China
[6]School of Physical Sciences, University of Chinese Academy of Sciences, No. 19A Yuquan Road, Beijing 100049, China
[7]CAS Key Laboratory of Theoretical Physics, Institute of Theoretical Physics, Chinese Academy of Sciences, Beijing 100190, China

(Received 6 November 2023; accepted 22 March 2024; published 18 April 2024)

The recent detection of a stochastic signal in the NANOGrav 15-year dataset has aroused great interest in uncovering its origin. However, the evidence for the Hellings-Downs correlations, a key signature of the gravitational-wave background (GWB) predicted by general relativity, remains inconclusive. In this paper, we search for an isotropic nontensorial GWB, allowed by general metric theories of gravity, in the NANOGrav 15-year dataset. Our analysis reveals a Bayes factor of approximately 2.5, comparing the quadrupolar (tensor transverse, TT) correlations to the scalar transverse (ST) correlations, suggesting that the ST correlations provide a comparable explanation for the observed stochastic signal in the NANOGrav data. We obtain the median and the 90% equal-tail amplitudes as $\mathcal{A}_{\rm ST} = 7.8^{+5.1}_{-3.5} \times 10^{-15}$ at the frequency of $1/\text{year}$. Furthermore, we find that the vector longitudinal (VL) and scalar longitudinal (SL) correlations are weakly and strongly disfavored by data, respectively, yielding upper limits on the amplitudes: $\mathcal{A}^{95\%}_{\rm VL} \lesssim 1.7 \times 10^{-15}$ and $\mathcal{A}^{95\%}_{\rm SL} \lesssim 7.4 \times 10^{-17}$. Lastly, we fit the NANOGrav data with the general transverse (GT) correlations parametrized by a free parameter α. Our analysis yields $\alpha = 1.74^{+1.18}_{-1.41}$, thus excluding both the TT ($\alpha = 3$) and ST ($\alpha = 0$) models at the 90% confidence level.

DOI: 10.1103/PhysRevD.109.084045

I. INTRODUCTION

A pulsar timing array (PTA) is dedicated to the detection of gravitational waves (GWs) with frequencies in the nanohertz range by regularly monitoring the spatially correlated fluctuations caused by GWs on the time of arrivals (TOAs) of radio pulses emitted by an array of pulsars [1–3]. There are three major PTA projects: the European PTA (EPTA) [4], the North American Nanoherz Observatory for GWs (NANOGrav) [5], and the Parkes PTA (PPTA) [6]. Over the course of more than a decade, these projects have been monitoring the TOAs from dozens of millisecond pulsars with an observation cadence ranging from weekly to monthly. These PTAs along with the Indian PTA (InPTA) [7] constitute the International PTA (IPTA) [8,9]. Meanwhile, the Chinese PTA (CPTA) [10] and the MeerKAT PTA (MPTA) [11] are relatively new PTA collaborations that use the sensitive new telescopes, FAST and MeerKAT.

Recently, NANOGrav [12,13], EPTA + InPTA [14,15], PPTA [16,17], and CPTA [18] have independently announced compelling evidence for a stochastic signal in their latest datasets. These datasets demonstrate varying levels of significance in supporting the presence of Hellings-Downs (HD) [19] spatial correlations as predicted by general relativity. While the PTA window covers a broad range of possible sources [20–33], the exact origin of the observed signal remains under active investigation, whether from astrophysical phenomena or cosmological processes [34–42]. A variety of sources can potentially explain the PTA signal [43–45], including the GW background (GWB) generated by supermassive black hole binaries [46–48], domain walls [49,50], cosmic strings [51–53], phase transitions [54–58], and scalar-induced GWs [59–65] accompanying the formation of primordial black holes [66–68].

*Corresponding author: ymwu@ucas.ac.cn
†Corresponding author: biyanchen@itp.ac.cn
‡Corresponding author: huangqg@itp.ac.cn
§zuchengchen@hunnu.edu.cn

Identifying a GWB as predicted by general relativity hinges on the observation of its quintessential quadrupolar characteristics, specifically the HD spatial correlations within PTA data. To achieve this goal, it is crucial to conduct a consistency test to confirm that the signal exhibits clearly quadrupolar characteristics [69], thereby ruling out other reasonable explanations such as the monopolar or dipolar correlations. While the NANOGrav 15-year dataset strongly disfavors individual monopole and dipole signals and exhibits a slight disfavoring tendency toward HD + monopole and HD + dipole models [13], it is important to note that this does not exclude the possibility of alternative GW polarization modes allowed in general metric theories of gravity. In fact, a most general metric gravity theory can have two scalar modes and two vector modes in addition to the two tensor modes, each with distinct correlation patterns [70–75]. It is worth noting that earlier studies [76–79] have tentatively reported evidence for scalar transverse (ST) correlations. To determine whether the observed PTA signal indeed originates from a GWB as predicted by general relativity, it is imperative to fit the data with all plausible correlation patterns. In this paper, we perform the Bayesian search for the stochastic GWB signal, modeled by a power-law spectrum with a varying power-law index. Our analysis considers all six polarization modes in the NANOGrav 15-year dataset.

II. DETECTING NONTENSORIAL GWBS WITH PTAS

Pulsar timing experiments take advantage of the regular arrival rates of radio pulses emitted by extremely stable millisecond pulsars. GWs can perturb the geodesics of these radio waves, leading to fluctuations in the TOAs of radio pulses [1,2]. The presence of a GW will result in unexplained residuals in the TOAs, even after compensating for a deterministic timing model that accounts for the pulsar spin behavior and the geometric effects caused by the motion of the pulsar and the Earth [1,2]. Through regularly monitoring TOAs of pulsars from an array of the highly stable millisecond pulsars [3], and analyzing the expected cross-correlations among pulsars in a PTA, it becomes possible to extract the GW signal from other systematic effects, such as the clock errors.

The cross-power spectral density of timing residuals induced by a GWB at the frequency f for two pulsars, a and b, can be expressed as [70–72]

$$S_{ab}(f) = \sum_P \frac{h^2_{c,P}}{12\pi^2 f^3} \Gamma^P_{ab}(f). \tag{1}$$

Here, $h^P_c(f)$ represents the characteristic strain, and the summation encompasses all six possible GW polarizations that can be inherent in a general metric gravity theory, specifically denoted as $P = +, \times, x, y, l, b$. The symbols "+" and "×" refer to the two spin-2 transverse traceless polarization modes; "x" and "y" correspond to the two spin-1 shear modes; "l" designates the spin-0 longitudinal mode; and "b" identifies the spin-0 breathing mode. The overlap reduction function (ORF) Γ^P_{ab} for a pair of pulsars is given by [70,71]

$$\Gamma^P_{ab}(f) = \frac{3}{8\pi} \int d\hat{\Omega} (e^{2\pi i f L_a (1+\hat{\Omega}\cdot\hat{p}_a)} - 1) \times (e^{2\pi i f L_b (1+\hat{\Omega}\cdot\hat{p}_b)} - 1) F^P_a(\hat{\Omega}) F^P_b(\hat{\Omega}), \tag{2}$$

where $\hat{p}$ is the direction of the pulsar with respect to the Earth, L_a and L_b are the distance from the Earth to the pulsar a and b respectively, and $\hat{\Omega}$ is the propagating direction of the GW. Additionally, antenna patterns $F^P(\hat{\Omega})$ are expressed as

$$F^P(\hat{\Omega}) = e^P_{ij}(\hat{\Omega}) \frac{\hat{p}^i \hat{p}^j}{2(1+\hat{\Omega}\cdot\hat{p})}, \tag{3}$$

where e^P_{ij} stands for the polarization tensor corresponding to polarization mode P [70,71]. As per the conventions established in [80], we define

$$\Gamma^{\mathrm{TT}}_{ab}(f) = \Gamma^{+}_{ab}(f) + \Gamma^{\times}_{ab}(f), \tag{4}$$

$$\Gamma^{\mathrm{ST}}_{ab}(f) = \Gamma^{b}_{ab}(f), \tag{5}$$

$$\Gamma^{\mathrm{VL}}_{ab}(f) = \Gamma^{x}_{ab}(f) + \Gamma^{y}_{ab}(f), \tag{6}$$

$$\Gamma^{\mathrm{SL}}_{ab}(f) = \Gamma^{l}_{ab}(f). \tag{7}$$

For the tensor transverse (TT) and ST polarization modes, the ORFs exhibit a notable property of being nearly independent of both distance and frequency, which can be analytically computed by [19,70]

$$\Gamma^{\mathrm{TT}}_{ab}(f) = \frac{1}{2}(1+\delta_{ab}) + \frac{3}{2} k_{ab} \left(\ln k_{ab} - \frac{1}{6} \right), \tag{8}$$

$$\Gamma^{\mathrm{ST}}_{ab}(f) = \frac{1}{8}(3 + 4\delta_{ab} + \cos\zeta_{ab}), \tag{9}$$

where δ_{ab} represents the Kronecker delta symbol, ζ_{ab} denotes the angular separation between pulsars a and b, and $k_{ab} \equiv (1-\cos\zeta_{ab})/2$. Note that $\Gamma^{\mathrm{TT}}_{ab}$ is commonly referred to as HD correlations, which are closely associated with the quadrupolar nature of GW signals. In contrast, analytical expressions for the vector longitudinal (VL) and scalar longitudinal (SL) polarization modes are not readily available. Therefore, we rely on numerical methods to compute these functions. In this work, we adopt the pulsar distance information collected in Table 2 of [81] to estimate the ORFs. It is worth noting that the ORFs for TT and ST

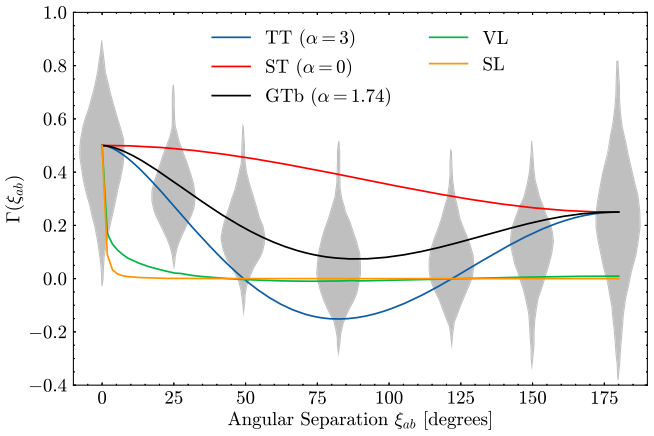

FIG. 1. Various ORFs examined in this work. Here, the GTb model refers to the GT model with $\alpha = 1.74$. The Bayesian reconstruction of normalized inter-pulsar correlations, as adapted from NANOGrav's analysis [13], is depicted by the gray violins. It is important to emphasize that the longitudinal modes, VL and SL, depend on both pulsar distance and GW frequency. The illustration here specifically presents the scenario where $fL_a = fL_b = 100$ for the VL and SL modes.

polarization modes only differ by the presence or absence of the term $\kappa_{ab} \ln \kappa_{ab}$. To generalize these ORFs, we adopt a parametrized form, following a similar approach as described in [79],

$$\Gamma_{ab} = \frac{1}{8}(3 + 4\delta_{ab} + \cos\xi_{ab}) + \frac{\alpha}{2}\kappa_{ab}\ln\kappa_{ab}. \quad (10)$$

Here, the parameter α allows us to seamlessly transition between the TT mode (when $\alpha = 3$) and the ST mode (when $\alpha = 0$). For later convenience, we refer to this parametrization as the "general transverse" (GT). See Fig. 1 for a visualization of various ORFs considered in this work.

Since current PTA data is not able to distinguish between various spectral shapes of the GWB energy density [34,43], we employ a power-law energy density spectrum in our analysis. This leads to the following expression:

$$S_{ab}(f) = \sum_{I=\mathrm{TT,ST,VL,SL}} \Gamma^I_{ab} \frac{\mathcal{A}_I^2}{12\pi^2}\left(\frac{f}{f_{\mathrm{yr}}}\right)^{-\gamma_I} f_{\mathrm{yr}}^{-3}, \quad (11)$$

where $\mathcal{A}_I$ is the GWB amplitude of polarization mode I, $f_{\mathrm{yr}} = 1/\mathrm{year}$, and γ_I corresponds to the spectral index for the polarization mode I that we treat as a free parameter. The dimensionless GW energy density parameter per logarithm frequency for the polarization mode I is related to $\mathcal{A}_I$ by, [82],

$$\Omega^I_{\mathrm{GW}}(f) = \frac{2\pi^2}{3H_0^2} f^2 h^2_{c,I} = \frac{2\pi^2 f_{\mathrm{yr}}^2}{3H_0^2}\mathcal{A}_I^2\left(\frac{f}{f_{\mathrm{yr}}}\right)^{5-\gamma_I}, \quad (12)$$

where $H_0 = 67.4\ \mathrm{km\,s^{-1}\,Mpc^{-1}}$ [83] is the Hubble constant.

III. DATA ANALYSIS

The NANOGrav 15-year dataset [12] comprises data from 68 pulsars. Following [13], we use 67 pulsars with timing baselines that exceed three years. The timing residuals for each pulsar, obtained by subtracting the timing model from the TOAs, can be expressed as [84]

$$\delta\boldsymbol{t} = M\boldsymbol{\epsilon} + F\boldsymbol{a} + \boldsymbol{n}. \quad (13)$$

The term $M\boldsymbol{\epsilon}$ serves to accommodate inaccuracies that can arise during the subtraction of the timing model, where M represents the design matrix of the timing model, and $\boldsymbol{\epsilon}$ is a vector that denotes minor deviations of the timing model parameters. The term $F\boldsymbol{a}$ encompasses all low-frequency signals, including both the red noise that is intrinsic to each pulsar and the common red noise signal shared among all pulsars, such as a GWB. Here, F corresponds to the Fourier design matrix, which features components of alternating sine and cosine functions. Given the timespan T, $\boldsymbol{a}$ is a vector that signifies the amplitude of the Fourier basis functions, and these functions are associated with specific frequencies of $\{1/T, 2/T, \ldots, N_{\mathrm{mode}}/T\}$. Similar to NANOGrav [13], we employ 30 frequency components to account for the intrinsic red noise specific to each pulsar, and these are characterized by a power-law spectrum. Additionally, we utilize 14 frequency components for the GWB signal. The final term $\boldsymbol{n}$ is responsible for modeling the timing residuals stemming from white noise, including a scale parameter on the TOA uncertainties (EFAC), an added variance (EQUAD), and a per-epoch variance (ECORR) for each backend/receiver system [84].

Similar to NANOGrav [13], we adopt the JPL solar system ephemeris (SSE) DE440 [85] as the fiducial SSE. Our Bayesian parameter inference follows a procedure closely aligned with the one outlined in [86,87]. The model parameters and their associated prior distributions are summarized in Table I. In our analyses, we keep the white noise parameters fixed at their maximum likelihood values to reduce the computational costs. We use ENTERPRISE [88] and ENTERPRISE_EXTENSION [89] software packages for the calculation of likelihood and Bayes factors. The Bayes factors are calculated using the *product-space* method [90–93]. For Markov chain Monte Carlo sampling, we utilize the PTMCMCSAMPLER [94] package. To expedite the burn-in process for the chains, we employ samples drawn from empirical distributions to handle the red noise parameters of the pulsars. These distributions are constructed based on posteriors obtained from an initial Bayesian analysis that exclusively incorporates the pulsars' red noise, excluding any common red noise processes, as carried out in [87,95].

TABLE I. Parameters and their prior distributions used in the analyses.

Parameter	Description	Prior	Comments
	White Noise		
E_k	EFAC per backend/receiver system	Uniform [0, 10]	Single-pulsar analysis only
Q_k[s]	EQUAD per backend/receiver system	Log-uniform $[-8.5, -5]$	Single-pulsar analysis only
J_k[s]	ECORR per backend/receiver system	Log-uniform $[-8.5, -5]$	Single-pulsar analysis only
	Red Noise		
$A_{\rm RN}$	Red-noise power-law amplitude	Log-uniform $[-20, -11]$	One parameter per pulsar
$\gamma_{\rm RN}$	Red-noise power-law spectral index	Uniform [0, 7]	One parameter per pulsar
	GWB Process		
A_I	GWB amplitude of polarization I	Log-uniform $[-18, -11]$	One parameter for PTA
γ_I	Power-law index of polarization I	Uniform [0, 7]	One parameter for PTA

TABLE II. The Bayes factors for various models compared to the TT model that considers the full HD spatial correlations derived from the product-space method. Here, the GTb model stands for the GT model with $\alpha = 1.74$. For all models, we use the power-law spectrum for the GWB with a varied power-law index parameter. The digit in parentheses gives the uncertainty on the last quoted digit.

Model	ST	VL	SL	GTb	TT + ST	TT + VL	TT + SL	TT + Mono	GTb + Mono	TT + Mono + Dipole	GTb + Mono + Dipole
BF	0.40(3)	0.12(2)	0.002(1)	3.9(3)	0.943(5)	0.489(6)	0.266(4)	0.548(6)	2.3(6)	0.255(4)	0.26(6)

IV. RESULTS AND DISCUSSION

Table II summarizes the Bayes factors for different models compared to the TT model that incorporates the full HD spatial correlations. The Bayes factor of the ST model relative to the TT model is 0.40 ± 0.03, indicating that there is no statistically significant evidence supporting or refuting the ST correlations over the HD correlations in the NANOGrav 15-year dataset. We obtain the median and the 90% equal-tail amplitudes as $\mathcal{A}_{\rm ST} = 7.8^{+5.1}_{-3.5} \times 10^{-15}$ at the reference frequency of $f_{\rm yr}$. The posterior distributions for the amplitude $A_{\rm ST}$ and the power-law index $\gamma_{\rm ST}$ are illustrated in Fig. 2.

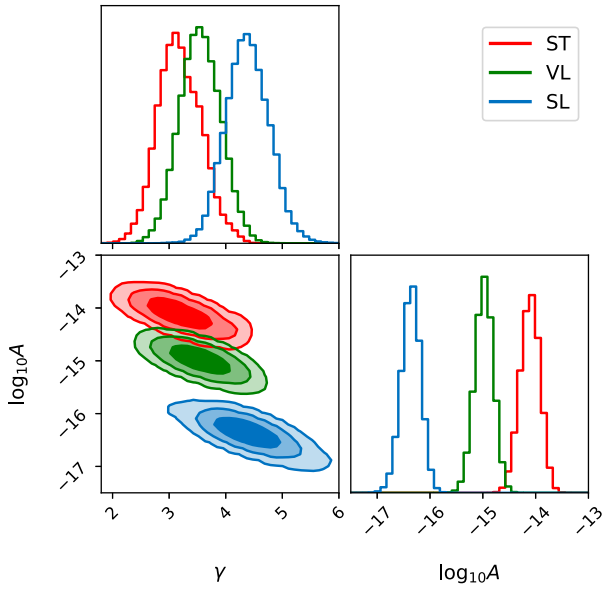

FIG. 2. Bayesian posteriors for the amplitude, A, and power-law index parameter, γ, obtained in the ST, VL, and SL models. We show the 1σ, 2σ, and 3σ contours in the two-dimensional plot.

The Bayes factor of the VL model versus the TT model is 0.12 ± 0.02, implying the VL correlations are slightly disfavored in comparison to the HD correlations. Furthermore, the Bayes factor of the SL model compared to the TT model is 0.002 ± 0.001, strongly disfavoring the SL correlations compared to the HD correlations. Consequently, we establish upper limits for the amplitudes as $\mathcal{A}_{\rm VL} \lesssim 1.7 \times 10^{-15}$ and $\mathcal{A}_{\rm SL} \lesssim 7.4 \times 10^{-17}$. Note that the constraint on the amplitude for the SL model is around two orders of magnitude tighter than that from other polarizations, mainly due to the strong autocorrelations inherent to the SL mode. The posteriors for the VL and SL models are also shown in Fig. 2. Notably, the power-law indexes derived from different polarizations, namely $\gamma_{\rm ST}$, $\gamma_{\rm VL}$, and $\gamma_{\rm SL}$, exhibit broad consistency. We also observe that the disfavored longitudinal modes remain slightly unfavorable when considered in combination with the TT mode. Specifically, we find $\mathrm{BF}^{\rm TT+VL}_{\rm TT} = 0.49$ and $\mathrm{BF}^{\rm TT+SL}_{\rm TT} = 0.27$.

We also consider a TT + ST model that simultaneously incorporates both the TT and ST correlations. The Bayes factor between the TT + ST model and the TT model is 0.943 ± 0.005, indicating that there is no significant evidence supporting or refuting the ST correlations in

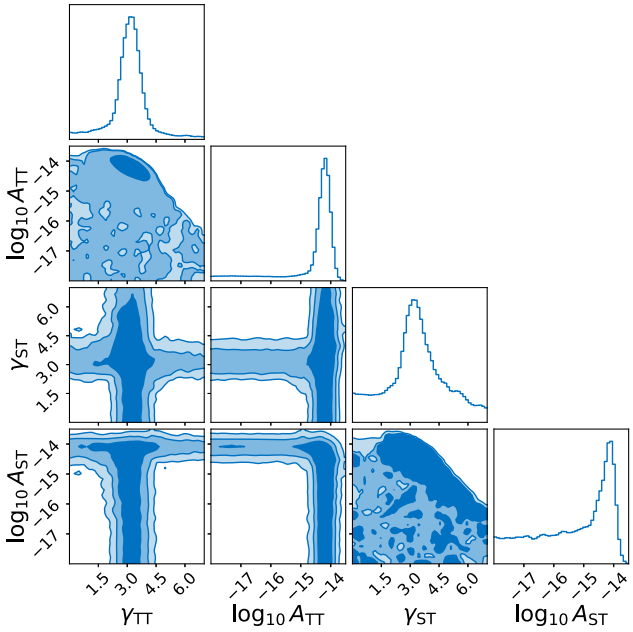

FIG. 3. Same as Fig. 2 but for the TT + ST model.

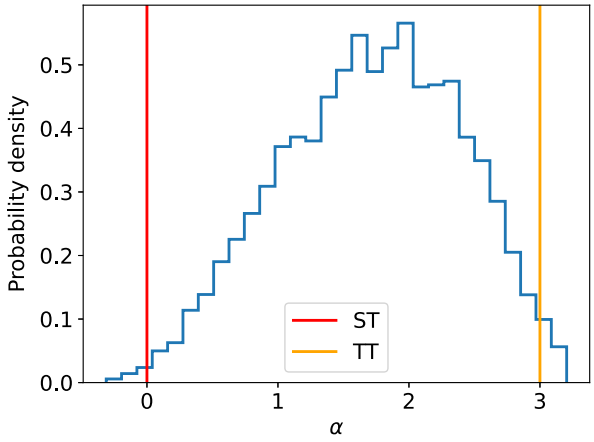

FIG. 4. Bayesian posteriors for the α parameter in the GT model with a parameterized ORF as defined by Eq. (10). The two vertical dashed lines correspond to the ST ($\alpha = 0$) and TT ($\alpha = 3$) ORFs, respectively.

addition to the HD correlations. The contour plot and the posterior distributions of the TT and ST components in the TT + ST model are depicted in Fig. 3. The presence of the peak around −14.5 for the amplitude $\log_{10} A_{\rm ST}$ confirms that the NANOGrav data do not rule out the possibility of an ST signal in the data.

To gain further insights into the optimal correlations that best describe the data, we also fit the NANOGrav 15-year dataset with a parametrized ORF (the GT model) as defined in Eq. (10). The posterior distribution for the free parameter α is displayed in Fig. 4. Our analysis yields a value of $\alpha = 1.74^{+1.18}_{-1.41}$, thus excluding both the TT and ST models at the 90% confidence level. However, it is worth noting that the TT and ST models remain consistent with the NANOGrav 15-year dataset at the 3σ confidence level. Furthermore, the Bayes factor between the GTb model, which is the GT model by fixing α to the best-fit value of 1.74, and the TT model is 3.9 ± 0.3, confirming that NANOGrav can be better described by the correlations with $\alpha \simeq 1.74$ than by the HD correlations with $\alpha = 3$. Furthermore, we calculate the Bayes factor comparing the TT + ST model and the GTb model as $\mathrm{BF}^{\rm TT+ST}_{\rm GTb} = 0.24$, indicating a preference for the GTb model over the TT + ST model.

More comprehensive model comparisons can be obtained when considering the presence of a monopole or dipole signal, as shown in both Table II and Table III. Particularly, from Table III, it is evident that even when accounting for these additional signals, the GTb model consistently outperforms other polarization models.

In summary, our analysis indicates that the NANOGrav 15-year dataset can be effectively described by either the TT correlations or the ST correlations, with no compelling evidence strongly favoring one over the other. The best-fitting model, GT with $\alpha \simeq 1.74$, might result from the potential impact of model misspecification, either in pulsar noise terms or the choice of model correlations. Nevertheless, the current PTA data cannot provide a definitive verdict on the spatial correlations within the stochastic signal, thereby posing a challenge for the unequivocal detection of the GWB predicted by general relativity through PTAs. Future work may need to consider the potential impact of cosmic variance in this quest [96–101]. We anticipate that future PTA data with a longer observation timespan and a larger number of pulsars will provide the necessary insights to pinpoint the origin of the observed stochastic signal.

It is noteworthy that the official NANOGrav collaboration independently conducted a study on transverse modes in their 15-year dataset, with their findings appearing on the arXiv shortly after ours [102]. Their analysis revealed strong Bayes factors supporting a correlated signal. Notably, the data did not exhibit a strong preference for either correlation signature, with Bayes factors around ∼2 when comparing TT to ST correlations and ∼1 for TT + ST correlations against TT correlations alone. These outcomes align closely with our findings, indicating robust consistency. However, certain differences between our analyses emerge. The official NANOGrav collaboration performed dropout analysis tests, which we did not undertake. They identified J0030 + 0451 and J0613–0200 as

TABLE III. The Bayes factors between various models by a conversion from Table II, e.g., $\mathrm{BF}^{\rm TT+ST}_{\rm GTb} = \mathrm{BF}^{\rm TT+ST}_{\rm TT}/\mathrm{BF}^{\rm GTb}_{\rm TT}$.

$\mathrm{BF}^{\rm TT+ST}_{\rm GTb}$	$\mathrm{BF}^{\rm TT+ST}_{\rm TT+mono}$	$\mathrm{BF}^{\rm GTb+mono}_{\rm TT+mono}$	$\mathrm{BF}^{\rm GTb+mono+dipole}_{\rm TT+mono+dipole}$
0.24	1.72	4.2	1.02

primarily responsible for the ST significance. Upon excluding these pulsars, they observed a significant increase in the Bayes factor for HD, accompanied by a notable reduction in the Bayes factor for ST. In contrast, our study extends beyond theirs by including searches for longitudinal polarization modes [VL in Eq. (6) and SL in Eq. (7)], aspects not explored in their analysis. Furthermore, we delved into a GT polarization mode characterized by the α parameter [see Eq. (10)], an avenue untouched by the official NANOGrav collaboration's investigation. Our findings indicate that the data can be best described by the GT correlations with $\alpha \simeq 1.74$.

Note added. A similar study by the NANOGrav collaboration [102], which explores transverse polarization modes in their 15-year dataset, was posted on arXiv one day after our manuscript. While the results regarding the ST mode from Ref. [102] are largely consistent with our findings, it is worth highlighting that our study investigates the SL, VL, and GT models that were not examined in Ref. [102].

ACKNOWLEDGMENTS

We acknowledge the use of the HPC Cluster of ITP-CAS. Q. G. H. is supported by grants from NSFC (Grant No. 12250010, No. 11975019, No. 11991052, No. 12047503), Key Research Program of Frontier Sciences, CAS, Grant No. ZDBS-LY-7009, the Key Research Program of the Chinese Academy of Sciences (Grant No. XDPB15). Z. C. C. is supported by the National Natural Science Foundation of China (Grant No. 12247176 and No. 12247112) and the China Postdoctoral Science Foundation Fellowship No. 2022M710429.

[1] M. V. Sazhin, Opportunities for detecting ultralong gravitational waves, Sov. Astron. **22**, 36 (1978).
[2] Steven L. Detweiler, Pulsar timing measurements and the search for gravitational waves, Astrophys. J. **234**, 1100 (1979).
[3] R. S. Foster and D. C. Backer, Constructing a pulsar timing array, Astrophys. J. **361**, 300 (1990).
[4] Michael Kramer and David J. Champion (EPTA Collaboration), The European pulsar timing array and the large European array for pulsars, Classical Quantum Gravity **30**, 224009 (2013).
[5] Maura A. McLaughlin, The North American nanohertz observatory for gravitational waves, Classical Quantum Gravity **30**, 224008 (2013).
[6] R. N. Manchester *et al.*, The Parkes pulsar timing array project, Pub. Astron. Soc. Aust. **30**, 17 (2013).
[7] Bhal Chandra Joshi, Prakash Arumugasamy, Manjari Bagchi *et al.*, Precision pulsar timing with the ORT and the GMRT and its applications in pulsar astrophysics, J. Astrophys. Astron. **39**, 51 (2018).
[8] G. Hobbs *et al.*, The international pulsar timing array project: Using pulsars as a gravitational wave detector, Classical Quantum Gravity **27**, 084013 (2010).
[9] R. N. Manchester, The international pulsar timing array, Classical Quantum Gravity **30**, 224010 (2013).
[10] K. J. Lee, Prospects of gravitational wave detection using pulsar timing array for Chinese future telescopes, in *Frontiers in Radio Astronomy and FAST Early Sciences Symposium 2015*, Astronomical Society of the Pacific Conference Series Vol. 502, edited by L. Qain and D. Li (Astronomical Society of the Pacific, 2016), p. 19, http://aspbooks.org/custom/publications/paper/502-0019.html.
[11] Matthew T. Miles *et al.*, The MeerKAT pulsar timing array: First data release, Mon. Not. R. Astron. Soc. **519**, 3976 (2023).
[12] Gabriella Agazie *et al.* (NANOGrav Collaboration), The NANOGrav 15 yr data set: Observations and timing of 68 millisecond pulsars, Astrophys. J. Lett. **951**, L9 (2023).
[13] Gabriella Agazie *et al.* (NANOGrav Collaboration), The NANOGrav 15 yr data set: Evidence for a gravitational-wave background, Astrophys. J. Lett. **951**, L8 (2023).
[14] J. Antoniadis *et al.* (EPTA Collaboration), The second data release from the European pulsar timing array—I. The dataset and timing analysis, Astron. Astrophys. **678**, A48 (2023).
[15] J. Antoniadis *et al.* (EPTA and InPTA Collaborations), The second data release from the European pulsar timing array—III. Search for gravitational wave signals, Astron. Astrophys. **678**, A50 (2023).
[16] Andrew Zic *et al.*, The parkes pulsar timing array third data release, Pub. Astron. Soc. Aust. **40**, e049 (2023).
[17] Daniel J. Reardon *et al.*, Search for an isotropic gravitational-wave background with the Parkes pulsar timing array, Astrophys. J. Lett. **951**, L6 (2023).
[18] Heng Xu *et al.*, Searching for the nano-hertz stochastic gravitational wave background with the Chinese pulsar timing array data release I, Res. Astron. Astrophys. **23**, 075024 (2023).
[19] R. w. Hellings and G. s. Downs, Upper limits on the isotropic gravitational radiation background from pulsar timing analysis, Astrophys. J. Lett. **265**, L39 (1983).
[20] Jun Li, Zu-Cheng Chen, and Qing-Guo Huang, Measuring the tilt of primordial gravitational-wave power spectrum from observations, Sci. China Phys. Mech. Astron. **62**, 110421 (2019);**64**, 250451(E) (2021).
[21] Zu-Cheng Chen, Chen Yuan, and Qing-Guo Huang, Pulsar timing array constraints on primordial black holes with NANOGrav 11-year dataset, Phys. Rev. Lett. **124**, 251101 (2020).

[22] Sunny Vagnozzi, Implications of the NANOGrav results for inflation, Mon. Not. R. Astron. Soc. **502**, L11 (2021).
[23] Micol Benetti, Leila Lobato Graef, and Sunny Vagnozzi, Primordial gravitational waves from NANOGrav: A broken power-law approach, Phys. Rev. D **105**, 043520 (2022).
[24] Zu-Cheng Chen, Yu-Mei Wu, and Qing-Guo Huang, Search for the gravitational-wave background from cosmic strings with the Parkes pulsar timing array second data release, Astrophys. J. **936**, 20 (2022).
[25] Amjad Ashoorioon, Kazem Rezazadeh, and Abasalt Rostami, NANOGrav signal from the end of inflation and the LIGO mass and heavier primordial black holes, Phys. Lett. B **835**, 137542 (2022).
[26] Yu-Mei Wu, Zu-Cheng Chen, Qing-Guo Huang, Xingjiang Zhu, N. D. Ramesh Bhat, Yi Feng, George Hobbs, Richard N. Manchester, Christopher J. Russell, and R. M. Shannon (PPTA Collaboration), Constraining ultralight vector dark matter with the Parkes pulsar timing array second data release, Phys. Rev. D **106**, L081101 (2022).
[27] Yu-Mei Wu, Zu-Cheng Chen, and Qing-Guo Huang, Search for stochastic gravitational-wave background from massive gravity in the NANOGrav 12.5-year dataset, Phys. Rev. D **107**, 042003 (2023).
[28] M. Falxa *et al.* (IPTA Collaboration), Searching for continuous gravitational waves in the second data release of the international pulsar timing array, Mon. Not. R. Astron. Soc. **521**, 5077 (2023).
[29] Yu-Mei Wu, Zu-Cheng Chen, and Qing-Guo Huang, Pulsar timing residual induced by ultralight tensor dark matter, J. Cosmol. Astropart. Phys. 09 (2023) 021.
[30] Virgile Dandoy, Valerie Domcke, and Fabrizio Rompineve, Search for scalar induced gravitational waves in the international pulsar timing array data release 2 and NANOgrav 12.5 years datasets, SciPost Phys. Core **6**, 060 (2023).
[31] Eric Madge, Enrico Morgante, Cristina Puchades-Ibáñez, Nicklas Ramberg, Wolfram Ratzinger, Sebastian Schenk, and Pedro Schwaller, Primordial gravitational waves in the nano-Hertz regime and PTA data—towards solving the GW inverse problem, J. High Energy Phys. 10 (2023) 171.
[32] Yan-Chen Bi, Yu-Mei Wu, Zu-Cheng Chen, and Qing-Guo Huang, Constraints on the velocity of gravitational waves from NANOGrav 15-year data set, arXiv:2310.08366.
[33] Yu-Mei Wu, Zu-Cheng Chen, Yan-Chen Bi, and Qing-Guo Huang, Constraining the graviton mass with the NANOGrav 15 year data set, Classical Quantum Gravity **41**, 075002 (2024).
[34] Adeela Afzal *et al.* (NANOGrav Collaboration), The NANOGrav 15 yr data set: Search for signals from new physics, Astrophys. J. Lett. **951**, L11 (2023).
[35] J. Antoniadis *et al.* (EPTA Collaboration), The second data release from the European pulsar timing array: V. Implications for massive black holes, dark matter and the early Universe, arXiv:2306.16227.
[36] Stephen F. King, Danny Marfatia, and Moinul Hossain Rahat, Toward distinguishing Dirac from Majorana neutrino mass with gravitational waves, Phys. Rev. D **109**, 035014 (2024).
[37] Xuce Niu and Moinul Hossain Rahat, NANOGrav signal from axion inflation, Phys. Rev. D **108**, 115023 (2023).
[38] Ido Ben-Dayan, Utkarsh Kumar, Udaykrishna Thattarampilly, and Amresh Verma, Probing the early Universe cosmology with NANOGrav: Possibilities and limitations, Phys. Rev. D **108**, 103507 (2023).
[39] Sunny Vagnozzi, Inflationary interpretation of the stochastic gravitational wave background signal detected by pulsar timing array experiments, J. High Energy Astrophys. **39**, 81 (2023).
[40] Chengjie Fu, Jing Liu, Xing-Yu Yang, Wang-Wei Yu, and Yawen Zhang, Explaining pulsar timing array observations with primordial gravitational waves in parity-violating gravity, Phys. Rev. D **109**, 063526 (2024).
[41] G. Agazie *et al.* (International Pulsar Timing Array Collaboration), Comparing recent PTA results on the nanohertz stochastic gravitational wave background, arXiv:2309.00693.
[42] Spyros Basilakos, Dimitri V. Nanopoulos, Theodoros Papanikolaou, Emmanuel N. Saridakis, and Charalampos Tzerefos, Induced gravitational waves from flipped SU(5) superstring theory at nHz, Phys. Lett. B **849**, 138446 (2024).
[43] Yu-Mei Wu, Zu-Cheng Chen, and Qing-Guo Huang, Cosmological interpretation for the stochastic signal in pulsar timing arrays, Sci. China Phys. Mech. Astron. **67**, 240412 (2024).
[44] John Ellis, Malcolm Fairbairn, Gabriele Franciolini, Gert Hütsi, Antonio Iovino, Marek Lewicki, Martti Raidal, Juan Urrutia, Ville Vaskonen, and Hardi Veermäe, What is the source of the PTA GW signal?, Phys. Rev. D **109**, 023522 (2024).
[45] Daniel G. Figueroa, Mauro Pieroni, Angelo Ricciardone, and Peera Simakachorn, Cosmological background interpretation of pulsar timing array data, arXiv:2307.02399.
[46] Gabriella Agazie *et al.* (NANOGrav Collaboration), The NANOGrav 15 yr data set: Constraints on supermassive black hole binaries from the gravitational-wave background, Astrophys. J. Lett. **952**, L37 (2023).
[47] John Ellis, Malcolm Fairbairn, Gert Hütsi, Juhan Raidal, Juan Urrutia, Ville Vaskonen, and Hardi Veermäe, Gravitational waves from supermassive black hole binaries in light of the NANOGrav 15-year data, Phys. Rev. D **109**, L021302 (2024), arXiv:2306.17021 [astro-ph.CO].
[48] Yan-Chen Bi, Yu-Mei Wu, Zu-Cheng Chen, and Qing-Guo Huang, Implications for the supermassive black hole binaries from the NANOGrav 15-year data set, Sci. China Phys. Mech. Astron. **66**, 120402 (2023).
[49] Naoya Kitajima, Junseok Lee, Kai Murai, Fuminobu Takahashi, and Wen Yin, Gravitational waves from domain wall collapse, and application to nanohertz signals with QCD-coupled axions, Phys. Lett. B **851**, 138586 (2024).
[50] E. Babichev, D. Gorbunov, S. Ramazanov, R. Samanta, and A. Vikman, NANOGrav spectral index $\gamma = 3$ from melting domain walls, Phys. Rev. D **108**, 123529 (2023).
[51] Naoya Kitajima and Kazunori Nakayama, Nanohertz gravitational waves from cosmic strings and dark photon dark matter, Phys. Lett. B **846**, 138213 (2023).

[52] John Ellis, Marek Lewicki, Chunshan Lin, and Ville Vaskonen, Cosmic superstrings revisited in light of NANOGrav 15-year data, Phys. Rev. D **108**, 103511 (2023).
[53] Waqas Ahmed, Talal Ahmed Chowdhury, Salah Nasri, and Shaikh Saad, Gravitational waves from metastable cosmic strings in the Pati-Salam model in light of new pulsar timing array data, Phys. Rev. D **109**, 015008 (2024).
[54] Andrea Addazi, Yi-Fu Cai, Antonino Marciano, and Luca Visinelli, Have pulsar timing array methods detected a cosmological phase transition?, Phys. Rev. D **109**, 015028 (2024).
[55] Peter Athron, Andrew Fowlie, Chih-Ting Lu, Lachlan Morris, Lei Wu, Yongcheng Wu, and Zhongxiu Xu, Can supercooled phase transitions explain the gravitational wave background observed by pulsar timing arrays?, arXiv:2306.17239.
[56] Yang Xiao, Jin Min Yang, and Yang Zhang, Implications of nano-Hertz gravitational waves on electroweak phase transition in the singlet dark matter model, Sci. Bull. **68**, 3158 (2023).
[57] Katsuya T. Abe and Yuichiro Tada, Translating nano-Hertz gravitational wave background into primordial perturbations taking account of the cosmological QCD phase transition, Phys. Rev. D **108**, L101304 (2023).
[58] Yann Gouttenoire, First-order phase transition interpretation of pulsar timing array signal is consistent with solar-mass black holes, Phys. Rev. Lett. **131**, 171404 (2023).
[59] Gabriele Franciolini, Antonio Iovino, Junior., Ville Vaskonen, and Hardi Veermae, Recent gravitational wave observation by pulsar timing arrays and primordial black holes: The importance of non-Gaussianities, Phys. Rev. Lett. **131**, 201401 (2023).
[60] Jia-Heng Jin, Zu-Cheng Chen, Zhu Yi, Zhi-Qiang You, Lang Liu, and You Wu, Confronting sound speed resonance with pulsar timing arrays, J. Cosmol. Astropart. Phys. 09 (2023) 016.
[61] Lang Liu, Zu-Cheng Chen, and Qing-Guo Huang, Probing the equation of state of the early Universe with pulsar timing arrays, J. Cosmol. Astropart. Phys. 11 (2023) 071.
[62] Zhu Yi, Zhi-Qiang You, You Wu, Zu-Cheng Chen, and Lang Liu, Exploring the NANOGrav signal and planet-mass primordial black holes through Higgs inflation, arXiv:2308.14688.
[63] Keisuke Harigaya, Keisuke Inomata, and Takahiro Terada, Induced gravitational waves with kination era for recent pulsar timing array signals, Phys. Rev. D **108**, 123538 (2023).
[64] Lang Liu, Zu-Cheng Chen, and Qing-Guo Huang, Implications for the non-Gaussianity of curvature perturbation from pulsar timing arrays, Phys. Rev. D **109**, L061301 (2024).
[65] Lang Liu, You Wu, and Zu-Cheng Chen, Simultaneously probing the sound speed and equation of state of the early Universe with pulsar timing arrays, arXiv:2310.16500.
[66] Zu-Cheng Chen and Qing-Guo Huang, Merger rate distribution of primordial-black-hole binaries, Astrophys. J. **864**, 61 (2018).
[67] M. Bousder, A. Riadsolh, A. El Fatimy, M. El Belkacemi, and H. Ez-Zahraouy, Implications of the NANOGrav results for primordial black holes and Hubble tension, arXiv:2307.10940.
[68] Yann Gouttenoire, Sokratis Trifinopoulos, Georgios Valogiannis, and Miguel Vanvlasselaer, Scrutinizing the primordial black holes interpretation of PTA gravitational waves and JWST early galaxies, arXiv:2307.01457.
[69] Bruce Allen, Sanjeev Dhurandhar, Yashwant Gupta, Maura McLaughlin, Priyamvada Natarajan, Ryan M. Shannon, Eric Thrane, and Alberto Vecchio, The international pulsar timing array checklist for the detection of nanohertz gravitational waves, arXiv:2304.04767.
[70] K. J. Lee, F. A. Jenet, and Richard H. Price, Pulsar timing as a probe of non-Einsteinian polarizations of gravitational waves, Astrophys. J. **685**, 1304 (2008).
[71] Sydney J. Chamberlin and Xavier Siemens, Stochastic backgrounds in alternative theories of gravity: Overlap reduction functions for pulsar timing arrays, Phys. Rev. D **85**, 082001 (2012).
[72] Jonathan R. Gair, Joseph D. Romano, and Stephen R. Taylor, Mapping gravitational-wave backgrounds of arbitrary polarisation using pulsar timing arrays, Phys. Rev. D **92**, 102003 (2015).
[73] Adrian Boîtier, Shubhanshu Tiwari, Lionel Philippoz, and Philippe Jetzer, Pulse redshift of pulsar timing array signals for all possible gravitational wave polarizations in modified general relativity, Phys. Rev. D **102**, 064051 (2020).
[74] Reginald Christian Bernardo and Kin-Wang Ng, Looking out for the Galileon in the nanohertz gravitational wave sky, Phys. Lett. B **841**, 137939 (2023).
[75] Reginald Christian Bernardo and Kin-Wang Ng, Stochastic gravitational wave background phenomenology in a pulsar timing array, Phys. Rev. D **107**, 044007 (2023).
[76] Zu-Cheng Chen, Chen Yuan, and Qing-Guo Huang, Nontensorial gravitational wave background in NANOGrav 12.5-year data set, Sci. China Phys. Mech. Astron. **64**, 120412 (2021).
[77] Zaven Arzoumanian *et al.* (NANOGrav Collaboration), The NANOGrav 12.5-year data set: Search for non-Einsteinian polarization modes in the gravitational-wave background, Astrophys. J. Lett. **923**, L22 (2021).
[78] Yu-Mei Wu, Zu-Cheng Chen, and Qing-Guo Huang, Constraining the Polarization of gravitational waves with the Parkes pulsar timing array second data release, Astrophys. J. **925**, 37 (2022).
[79] Zu-Cheng Chen, Yu-Mei Wu, and Qing-Guo Huang, Searching for isotropic stochastic gravitational-wave background in the international pulsar timing array second data release, Commun. Theor. Phys. **74**, 105402 (2022).
[80] Neil J. Cornish, Logan O'Beirne, Stephen R. Taylor, and Nicolás Yunes, Constraining alternative theories of gravity using pulsar timing arrays, Phys. Rev. Lett. **120**, 181101 (2018).
[81] Gabriella Agazie *et al.* (NANOGrav Collaboration), The NANOGrav 15 yr data set: Bayesian limits on gravitational waves from individual supermassive black hole binaries, Astrophys. J. Lett. **951**, L50 (2023).
[82] Eric Thrane and Joseph D. Romano, Sensitivity curves for searches for gravitational-wave backgrounds, Phys. Rev. D **88**, 124032 (2013).

[83] N. Aghanim *et al.* (Planck Collaboration), Planck 2018 results. VI. Cosmological parameters, Astron. Astrophys. **641**, A6 (2020); **652**, C4(E) (2021).
[84] Z. Arzoumanian *et al.* (NANOGrav Collaboration), The NANOGrav nine-year data set: Limits on the isotropic stochastic gravitational wave background, Astrophys. J. **821**, 13 (2016).
[85] Ryan S. Park, William M. Folkner, James G. Williams, and Dale H. Boggs, The JPL planetary and lunar ephemerides de440 and de441, Astron. J. **161**, 105 (2021).
[86] Z. Arzoumanian *et al.* (NANOGRAV Collaboration), The NANOGrav 11-year data set: Pulsar-timing constraints on the stochastic gravitational-wave background, Astrophys. J. **859**, 47 (2018).
[87] Zaven Arzoumanian *et al.* (NANOGrav Collaboration), The NANOGrav 12.5 yr data set: Search for an isotropic stochastic gravitational-wave background, Astrophys. J. Lett. **905**, L34 (2020).
[88] Justin A. Ellis, Michele Vallisneri, Stephen R. Taylor, and Paul T. Baker, Enterprise: Enhanced numerical toolbox enabling a robust pulsar inference suite, Zenodo, 10.5281/zenodo.4059815 (2020).
[89] Stephen R. Taylor, Paul T. Baker, Jeffrey S. Hazboun, Joseph Simon, and Sarah J. Vigeland, enterprise_extensions, (2021), v2.2.0.
[90] Bradley P. Carlin and Siddhartha Chib, Bayesian model choice via markov chain monte carlo methods, J. R. Stat. Soc. Ser. B **57**, 473 (1995).
[91] Simon J. Godsill, On the relationship between Markov Chain Monte Carlo methods for model uncertainty, J. Comput. Graph. Stat. **10**, 230 (2001).
[92] Sonke Hee, Will Handley, Mike P. Hobson, and Anthony N. Lasenby, Bayesian model selection without evidences: Application to the dark energy equation-of-state, Mon. Not. R. Astron. Soc. **455**, 2461 (2016).
[93] Stephen R. Taylor, Rutger van Haasteren, and Alberto Sesana, From bright binaries to bumpy backgrounds: Mapping realistic gravitational wave skies with pulsar-timing arrays, Phys. Rev. D **102**, 084039 (2020).
[94] Justin Ellis and Rutger van Haasteren, jellis18/ptmcmcsampler: Official release, (2017).
[95] K. Aggarwal *et al.*, The NANOGrav 11-year data set: Limits on gravitational waves from individual supermassive black hole binaries, Astrophys. J. **880**, 116 (2019).
[96] Bruce Allen, Variance of the Hellings-Downs correlation, Phys. Rev. D **107**, 043018 (2023).
[97] Bruce Allen and Joseph D. Romano, Hellings and Downs correlation of an arbitrary set of pulsars, Phys. Rev. D **108**, 043026 (2023).
[98] Reginald Christian Bernardo and Kin-Wang Ng, Pulsar and cosmic variances of pulsar timing-array correlation measurements of the stochastic gravitational wave background, J. Cosmol. Astropart. Phys. 11 (2022) 046.
[99] Reginald Christian Bernardo and Kin-Wang Ng, Testing gravity with cosmic variance-limited pulsar timing array correlations, arXiv:2306.13593.
[100] Reginald Christian Bernardo and Kin-Wang Ng, Hunting the stochastic gravitational wave background in pulsar timing array cross correlations through theoretical uncertainty, J. Cosmol. Astropart. Phys. 08 (2023) 028.
[101] Reginald Christian Bernardo and Kin-Wang Ng, Beyond the Hellings-Downs curve: Non-Einsteinian gravitational waves in pulsar timing array correlations, arXiv:2310.07537.
[102] Gabriella Agazie *et al.* (NANOGrav Collaboration), The NANOGrav 15-year data set: Search for transverse polarization modes in the gravitational-wave background, Astrophys. J. Lett. **964**, L14 (2024).